Behavior of the Deeply Inserted Helices in Diphtheria Toxin T Domain: Helices 5, 8, and 9 Interact Strongly and Promote Pore Formation, While Helices 6/7 Limit Pore Formation[†]

Bing Lai, Gang Zhao, and Erwin London*

Department of Biochemistry and Cell Biology, Stony Brook University, Stony Brook, New York 11794-5215

Received December 21, 2007; Revised Manuscript Received January 30, 2008

ABSTRACT: Diphtheria toxin T domain aids the membrane translocation of diphtheria toxin A chain. When the isolated T domain is deeply membrane-inserted, helices TH 8−9 form a transmembrane hairpin, while helices TH 5−7 form a deeply inserted nontransmembrane structure. Blocking deep insertion of TH 8−9 blocks deep insertion of TH 5−7 (Zhao, G., and London, E. (2005) *Biochemistry 44*, 4488–4498). We now examine the effects of blocking the deep insertion of TH 5 and TH 6/7. An A282R/V283R dual substitution in TH 5 prevented its deep insertion, significantly decreased the deep insertion of TH 9, and to a lesser degree that of TH 6/7. Blocking deep insertion of TH 6/7 with a L307R mutation had no effect on the deep insertion of TH 5, similar to its previously characterized lack of effect on the deep insertion of TH 8−9. An I364K mutation in TH 9 blocked TH 8−9 deep insertion and greatly reduced pore formation by the T domain, consistent with the role of TH 8−9 in pore formation. The A282R/V283R mutations also reduced the extent of pore formation, but to a lesser degree, suggesting either that TH 5 is part of the pore or that interactions with TH 5 affect the ability of TH 8−9 to form pores. The L307R mutation *enhanced* the extent of pore formation, suggesting that deeply inserted TH 6/7 may act as a "cork" that partly blocks the pore. Combined, these results indicate that TH 5, 8, and 9 combine to form a deeply inserted scaffold of more strongly associated helices.

Diphtheria toxin (DT[1]), a protein secreted by *Corynebacterium diphtheriae*, is composed of two polypeptide chains, A and B, connected by a disulfide bond. This 535-residue toxin is one of the most thoroughly studied bacterial toxins. Crystallography reveals that DT has three distinct domains (*1–3*). The catalytic (C) domain is equivalent to the A chain. The B chain contains the other two domains: the receptor binding (R) domain and the transmembrane (T) domain. The R domain binds to the cell surface receptor, after which the toxin undergoes endocytosis. When DT reaches the low pH environment of the lumen of an endosome, it partially unfolds and inserts into the endosomal membrane (*4–8*). Aided by the T domain, the A chain is then translocated across the lipid bilayer, and after cleavage of the disulfide bond attaching it to the T domain, it is released into the cytoplasm (*9–11*). The released A chain catalyzes the ADP-ribosylation of the elongation factor-2 and thereby stops protein synthesis in the intoxicated cell (*12*).

The α-helical T domain plays a key role in membrane insertion and translocation (*13–19*). The crystal structure of the T domain reveals that it has 9 major α-helices, named TH1–9 (*1, 2*). In aqueous solution, the helices form three layers. The first layer, which is the most exposed to solution, contains the most hydrophilic helices, TH 1–4. The second layer contains TH 5−7, which are somewhat hydrophobic. The most hydrophobic helices, TH 8−9, form the third layer. At low pH, the T domain undergoes a partial unfolding event triggered to a significant degree by the protonation of His residues within the hydrophilic helices (*20*). Contact between the helices is disrupted such that the hydrophobic helices of the T domain become exposed to solution (*4, 21, 22*), and amphiphilic helix TH 1 twists so that its hydrophobic face is exposed (*23*). Thus, low pH primes the T domain for membrane penetration.

T domain helical structure remains intact when it inserts into the lipid bilayer (*21, 24*); therefore, changes in its conformation upon membrane insertion are likely to involve changes in the way the helices are arranged. Several studies have investigated the topography of the membrane-inserted T domain. The membrane conformation of TH 8−9 has been studied most thoroughly (*4, 24–29*). Upon insertion into model membrane vesicles at low pH (5.5 and below), TH 8−9 can form one of two states. One is the P state, in which TH 8−9 are shallowly bound near the membrane surface (*5, 28*). The other is TM state, in which TH 8−9 deeply insert in

[†] This work was supported by NIH Grant GM31986.

* Corresponding author. Phone: 631-632-8564. Fax: 631-632-8575. E-mail: Erwin.London@stonybrook.edu.

[1] Abbreviations: 10-DN, 10-doxylnonadecane; BODIPY, 4,4-difluoro-5,7-dimethyl-4-bora-3*a*,4*a*-diaza-*s*-indacene; BODIPY-IA, (*N*-(4,4-difluoro-5,7-dimethyl-4-bora-3*a*,4*a*-diaza-*s*-indacene-3-yl)methyl)iodoacetamide; BODIPY-SA, BODIPY-labeled streptavidin; DMoPC, dimyristoleoylphosphatidylcholine; DOPC, dioleoylphosphatidylcholine; DOPG, dioleoylphosphatidylglycerol; DT, diphtheria toxin; HSA, human serum albumin; IPTG, isopropyl-1-thio-β-D-thiogalactopyranoside; LUV, large unilamellar vesicles; P state, partially/shallowly inserted T domain state; SDS−PAGE, sodium dodecyl sulfate−polyacrylamide gel electrophoresis; SUV, small unilamellar vesicles; T domain, diphtheria toxin "transmembrane" domain; TCEP, Tris(2-carboxyethyl)phosphine; TM state, deeply inserted T domain state in which TH 8 and TH 9 form a transmembrane structure.

10.1021/bi7025134 CCC: $40.75
Published on Web 03/21/2008

the membrane and form a transmembrane hairpin (*5, 28*). Topography studies from our laboratory show that TH 5−7 also locate shallowly in the P state and are buried deeply within the bilayer in the TM state, but do not form a transmembrane structure in the TM state, at least in isolated T domain, while hydrophilic helices TH 1–3 remain shallow in both the P and TM states (*23, 30, 31*). This may mean that there are no strong interactions between the hydrophobic helices and TH 1–3 (*23*), and so at some stage of translocation, the hydrophilic helices of the T domain may simply loosely tether the A chain to the hydrophobic helices. However, at other stages, TH 1, which is somewhat amphiphilic, may form a TM structure (*22, 32*).

In both the P and TM states TH 1–7 remain predominantly on the cis (insertion) side of the membrane (*30, 31*). Thus, A chain attached to TH1 would be on the cis side of the membrane in these states, and these conformations correspond to pretranslocation states. Planar bilayer studies have identified a different "open channel" topography, in which TH 5 forms a transmembrane state, and TH 1–4 reach the trans (translocated) side of the lipid bilayer (*13, 16*). When the A chain is attached to the T domain in this state, it is also on the trans side of the membrane (*15*). Thus, this state appears to correspond to a post-translocation state.

In some fashion, the A chain translocation is thought to involve pore formation by the T domain. Pore formation studies in planar bilayers have found that TH 8−9 can form a pore without the aid of other parts of the T domain (*33*). Mutagenesis studies have been useful in analysis of pore formation (*16, 17, 27, 34–36*). For example, a Pro substitution that inhibits toxicity, at residue 345, blocks both proper T domain insertion and pore formation (*17*). Despite these studies, the precise nature of the linkage between pore formation and translocation is unclear. One complication is that the T domain may form a "sticky pore" with chaperone-like properties (*37, 38*). Another complication is that pore properties and structure may change markedly during translocation.

Mutagenesis has also proven useful to study T domain membrane topography (*5, 6, 16, 17, 25, 27, 28, 30, 31, 39*). Studies in model membrane vesicles show that in the pretranslocation TM state, mutations blocking the proper insertion of TH 8−9 also prevent deep insertion of TH 5 and TH 6/7 (*39*). However, blocking the insertion of TH 6/7 has no effect on the insertion of TH 8−9 (*39*).

Overall, T domain behavior in membranes is nonclassical for membrane proteins in terms of its topographical flexibility, unusual hydrophobic helix topographies, and hierarchy of interactions between different helices. We believe this complex behavior is a key clue to the mechanism of A chain translocation. In this article, we have used additional insertion-inhibiting mutations to extend studies of the helix interaction hierarchy. Cationic insertion-inhibiting mutations were introduced at residues 282 and 283 in TH 5, 307 in TH 6/7, or at 364 in TH 9. Fluorescently labeled cysteine point mutations were used to probe helix insertion. The results indicate that there is a distinct hierarchy of helix-helix interactions in the pretranslocation TM state and that TH 6/7 may play a previously unsuspected role in controlling pore formation in the pretranslocation state.

EXPERIMENTAL PROCEDURES

Materials. Dioleoylphosphatidylcholine (DOPC), dimyristoleoylphosphatidylcholine (DMoPC) and dioleoylphosphatidylglycerol (DOPG) were purchased from Avanti Polar Lipids (Alabaster, AL). Lissamine rhodamine B labeled 1,2-dihexadecanoyl-*sn*-glycero-3-phosphoethanolamine (rhodamine-DHPE), *N*-[(4,4-difluoro-5,7-dimethyl-4-bora-3*a*,4*a*-diaza-*s*-indecene-3-yl)methyl]iodoacetamide (BODIPY-FL C1-IA, BODIPY-IA), monochlorobimane, rabbit anti-BODIPY FL IgG, and BODIPY-IA labeled streptavidin (custom order) were purchased from Molecular Probes (Eugene, OR). Lipid concentrations were determined by dry weight. Human serum albumin (HSA) was from Worthington Biochemical (Lakewood, NJ). PCR supermix, endonucleases and T4 ligase were purchased from Invitrogen (Carlsbad, CA). Plasmid preparation and gel extraction kits were purchased from Qiagen (Valencia, CA). EN^{3}HANCE autoradiography enhancer was from PerkinElmer (Waltham, MA). All other chemicals were reagent grade.

PCR-Based Mutagenesis. The DNA sequence of the T domain attached to an N-terminal 20 residue His6-tag and inserted into the pET15b plasmid (*40*) was used for mutagenesis (T domain residues 203–378 attached to the N-terminal His6-tag are defined as the wild type (WT) T domain). A two-step PCR based mutagenesis method was used to produce T domain mutants. Primers were designed to produce a point mutation resulting in an amino acid substitution (or two mutations in consecutive amino acid codons). The internal 5′ and 3′ primers contained complementary sequences with 18 WT nucleotides upstream and 18 WT nucleotides downstream of the nearest mutated nucleotide.

PCR was performed using an Eppendorf Mastercycler PCR system (Westbury, NY) using regular Taq DNA polymerase. The first PCR step contained two parallel PCR reactions. One PCR reaction used a T7 promoter and the internal 3′ primer. The other reaction used the internal 5′ primer and a T7 terminator primer. The two reaction products were purified on agarose gels and mixed to form the template for the second PCR step. The second PCR used T7 promoter and T7 terminator as primers. The product was digested with XbaI and XhoI and ligated into pET28a plasmid linearized by the same restriction enzymes. The ligation product was transformed into XL-1 blue cells, kanamycin resistant clones were selected, and then plasmids were extracted and sequenced (Genewiz, South Plainfield, NJ) to confirm the desired mutation was obtained and that no additional mutations were present.

Expression and Purification of the T Domain. Mutant plasmids were used to transform competent *E. coli* BL21(DE3) cells, and then protein was expressed as described below. A single colony was picked to inoculate 25 mL Luria–Bertani media containing 30 μg/mL kanamycin. After overnight shaking at 37 °C, the culture was transferred to a 2 L flask and shaken for about 3 h at 37 °C. When the optical density at 600 nm reached 0.5, the culturing temperature was reduced to about 23 °C. When the optical density was 0.8, 0.25 g/L isopropyl-1-thio-β-D-thiogalactopyranoside was added to induce protein expression. After a 4 h of induction at 25 °C, a temperature chosen to increase expression levels, the cells were harvested by centrifugation and stored at −20 °C. The

cells were resuspended in 30 mL of binding buffer (20 mM Tris-Cl, pH 8.0, 150 mM NaCl, and 5 mM imidazole) containing 0.1 mg/mL hen egg white lysozyme. The suspension was incubated at room temperature for 30 min and then further disrupted by tip sonication (W-220F cell disruptor, Heat Systems, Ultrasonics, Inc., Plainview, NY) for 15 s while cooled on ice and then cooled a further 15 s. The sonication and cooling steps were repeated two times. The solution was centrifuged at 12,000*g* at 4 °C for 20 min, and the supernatant was collected. Then, 1 mL TALON metal affinity resin (Clontech Laboratories, Inc., Mountain View, CA) was added to the supernatant. The solution was gently agitated at room temperature for 20 min to allow the His6-tagged T domain mutant to bind to the resin. The protein-bound resin was collected and transferred to a 10 mL gravity-flow column. The column was washed by 10 mL binding buffer. The protein was then eluted with 3 mL elution buffer (20 mM Tris-Cl, pH 8.0, 150 mM NaCl, and 200 mM imidazole). The eluted sample was diluted to 50 mL with 20 mM Tris-Cl at pH 8.0 and loaded onto a Source Q anion-exchange column (Amersham Biosciences (Piscataway, NJ)). The column was eluted at a rate of 1 mL/min with an increasing NaCl gradient (20 mM Tris-Cl and 0–500 mM NaCl). The T domain peak appeared at about 300 mM NaCl. The protein was collected and subjected to SDS−PAGE to assay purity (which was >90%). Protein concentration was determined by Bradford method using the kit from BioRad (Hercules, CA). The purified protein was stored either at 4 °C for short periods (less than 1 week) or in a set of aliquots at −70 °C for long periods.

Fluorescence Labeling of the T Domain. T domain containing a Cys mutation was labeled with BODIPY-IA or monochlorobimane similarly to as described previously (*30*). To do this, 0.2 mg/mL protein was reduced with 100 mM dithiothreitol for 1 h and dialyzed overnight against 4 L TBS buffer (10 mM Tris-Cl, pH 8.0, and 150 mM NaCl) without a buffer change. BODIPY-IA dissolved in dimethylsulfoxide or monochlorobimane dissolved in ethanol were added to the protein solution to give a final probe/protein molar ratio of at least 10:1 (BODIPY-IA and monochlorobimane stock solution concentrations were ∼20 mM and ∼50 mM, respectively). For mutants that were difficult to label, the probe/protein ratio was increased to 40:1. The mixture was covered with aluminum foil and slowly agitated at room temperature for 1 h. Next, it was dialyzed overnight against 4 L TBS with one change of buffer. Relative labeling efficiency was determined by comparing the fluorescence of the labeled protein to that of WT protein lacking Cys treated using the same procedure. Fluorescence intensity of the protein containing a Cys was at least 8 times greater than the background labeling of T domain without Cys.

Fluorescence Measurements. Fluorescence was measured on a Spex tau-2 Fluorolog spectrofluorimeter operating in steady state mode. Fluorescence measurements were performed at room temperature using excitation and emission slit widths of 2.5 mm (band-pass 4.5 nm) and 5 mm (band-pass 9 nm), respectively. Semimicro quartz cuvettes with an excitation path length of 10 mm and emission path length of 4 mm were used. Trp was excited at 280 nm, and fluorescence emission was measured at 330 and 350 nm. For bimane fluorescence spectra, bimane was excited at 380 nm and emission measured over the range 420 to 500 nm. For measurements of bimane fluorescence at fixed wavelengths, the excitation wavelength was 380 nm, and the emission wavelength was at the emission maximum (in the absence of any quencher) for the labeled protein being studied. BODIPY fluorescence was excited at 488 nm and emission measured at 516 nm. The fluorescence from background samples lacking protein was also measured and subtracted from the reported values.

Lipid-Binding Experiments. The binding of the T domain mutants to lipid vesicles was measured using Trp fluorescence, which blue shifts upon binding (*25*). To do this, 3.5 μg of unlabeled T domain was added to 700 μL of Tris-acetate buffer (6.7 mM Tris-Cl, 167 mM acetate, and 150 mM NaCl, pH 4.5) and incubated for 20 min at room temperature. Then, aliquots of small unilamellar vesicles (SUV), prepared by sonication as described previously (*28*), and composed of 10 mM 70 mol % DOPC/30 mol % DOPG or 10 mM 70 mol % DMoPC/30 mol % DOPG dispersed in Tris-acetate buffer were titrated into the solution, with a 10 min incubation time after the addition of each aliquot of lipid. The ratio of the fluorescence emission intensity at 330 and 350 nm was recorded.

Preparation of Model Membrane-Incorporated T Domain. Stock SUV preparations contained 10 mM 70%DOPC/30%DOPG or 10 mM 70%DMoPC/30%DOPG (see above). Typically, a 16 μL aliquot of SUV was added to 780 μL of Tris-acetate buffer. To this, 4 μL of 200 μg/mL fluorescently labeled T domain was added to give a final protein concentration of 1 μg/mL, and the sample was then incubated at room temperature for 20 min. For bimane-labeled T domain, fluorescence was measured as described above. For the BODIPY-labeled T domain, anti-BODIPY antibody induced quenching was measured in a manner similar to that described previously (*30*). To do this, the initial fluorescence was measured, and then 20 μL of anti-BODIPY antibody (from a 3 mg/mL stock solution) was added to the sample. After 20 min of incubation at room temperature, the BODIPY fluorescence was remeasured.

In the experiments to examine the effect of high T domain concentration or the presence of HSA upon the behavior of the labeled T domain, bimane- or BODIPY-labeled T domain was incorporated into 70%DOPC/30%DOPG SUV as described above, and after 10 min of incubation, 5 μg/mL WT T domain (from a ∼1–2 mg/mL stock solution) or 5 μg/mL HSA (from a 1 mg/mL stock solution dissolved in 10 mM Tris-Cl pH 8.0) was added. Samples were then incubated for another 10 min, and the bimane or BODIPY fluorescence was measured.

Dual Quenching of the Bimane-Labeled Proteins. Dual quenching was used to detect the depth of the bimane-labeled residues in the lipid bilayers in a manner similar to that described previously (*41*). Briefly, iodide ion was used as the aqueous quencher, and 10-doxylnonadecane (10-DN) was used as the membrane-bound quencher. A SUV preparation was prepared by sonication in 5 mM Tris-Cl at pH 8. For the 10-DN containing samples, SUV contained 1 mM 10-DN and 10 mM 70%DOPC/30%DOPG or 0.78 mM 10-DN and 10 mM 70%DMoPC/30%DOPG. After dilution of the lipid to 201 μM 70%DOPC/30%DOPG or 70%DMoPC/30%DOPG with Tris-acetate at pH 4.5, a small aliquot of bimane-labeled T-domain (4 μL) was added to give 1 μg/mL bimane-labeled protein in a total volume of 800 μL and

a final lipid concentration of 200 μM. After a 20 min incubation, the fluorescence in the sample with 10-DN ($F_{10\text{-DN}}$) and without 10-DN (F_0) was measured. For iodide quenching experiments, bimane-labeled T domain was incorporated into SUV prepared without 10-DN as described above. Fluorescence was measured, before (F_0) and after (F_{KI}) the addition of 40 μL of 2 M KI containing 1 mM freshly prepared $Na_2S_2O_3$. The quenching radio was calculated from the formula $Q = Q_{10\text{-DN}}/Q_{KI} = ((F_0/F_{10\text{-DN}}) - 1)/((F_0/F_{KI}) - 1)$. A higher quenching ratio indicates a deeper burial of the bimane-labeled residue.

^{14}C-N-Ethylmaleimide Labeling of T Domain Cysteine Mutants. ^{14}C-NEM labeling was used as a control to examine whether mutations inhibited insertion of unlabeled proteins. A fresh ^{14}C-NEM stock solution was prepared by adding 100 μL of 3.01 mM ^{14}C-NEM (33.2 mCi/mmol) dissolved in pentane to 100 μL of Tris-acetate buffer. After evaporation of the pentane phase at room temperature (about 1 h), the solution was vortexed. Meanwhile, a sample containing 100μg/mL Cys-containing T domain mutant inserted into SUV composed of 2 mM 70%DMoPC/30%DOPG dispersed in Tris-acetate buffer at pH 4.5 was prepared in a volume of 100 μL. After incubation at room temperature for 20 min, 10 μL of the ^{14}C-NEM solution was added to the T domain sample to give 0.27 mM final ^{14}C-NEM concentration. The sample was then incubated at room temperature for either 2 or 24 h. To stop the reaction, 1 μL of 1 M dithiothreitol was added. After 5 min, 25 μL of 50 w/v % TCA was added, and the sample was incubated on ice for 20 min. After centrifugation at 16,000*g* for 1 min, the supernatant was removed, 20 μL of Laemmli sample loading buffer from Biorad (Hercules, CA) was added to the pellet, and then SDS−PAGE was performed using a 5% acrylamide/bis-acrylamide stacking gel/10% acrylamide/bis-acrylamide resolving gel. The gel was fixed in 30 v/v % methanol/10 v/v % acetic acid for 1 h and then treated with EN^{3}HANCE autoradiography enhancer for 1 h. It was then immersed in water and shaken for 30 min. Finally, the gel was dried on slab gel dryer Model SE1160 from Hoefer Scientific Instruments (San Francisco, CA) and exposed to a phosphor screen from GE Healthcare Bio-Sciences Corp. (Piscataway, NJ) for 12 h. The image was scanned with a STORM 840 system from GE Healthcare Bio-Sciences Corp. The ratio of the band intensity at 2 h to intensity at 24 h was used as a measure of the rate of reaction of a residue with NEM and thus its exposure to aqueous solution.

Concentration-Dependent Pore Formation. T domain-induced pore formation was measured in manner similar to that described previously (*39*). We modified the previous protocol by preincubating the T domain in 3.3 mM TCEP (from a 330 mM stock solution dissolved in Na-acetate at pH 6.5) for 20 min in order to reduce any disulfide bond formation. This was found to increase the level of pore formation to a significant degree. BODIPY-labeled streptavidin (BODIPY-SA) was trapped in LUV composed of 70%DOPC/30%DOPG dispersed in Tris-acetate at pH 4.5 as described previously (*31*). The final stock solution contained about 4 μg/mL BODIPY-SA and 4 mM lipid. LUV with trapped BODIPY-SA was diluted to 790 μL with Tris-acetate buffer at pH 4.5 to give a final lipid concentration of 100 μM lipid. Various concentrations of T domain in 5 μL of TBS were added to the samples. After a 20 min incubation, 3 μL of 8 μM biocytin in water was added to a give a 20-fold excess over the molar concentration of BODIPY-SA, and the increase in BODIPY fluorescence due to biocytin influx was monitored for 20 min.

RESULTS

Sites Chosen for T Domain Mutations. Site-directed mutagenesis was used to prepare T domains with charged substitutions known to or likely to prevent deep membrane insertion of hydrophobic helices. These mutations were introduced in TH 5 (A282R/V283R), TH 6/7 [which is a single hydrophobic segment broken into two helices by a Pro] (L307R), and TH 9 (I364K). To probe the effects of these mutations upon the topography of the hydrophobic helices of the T domain, single Cys residues were introduced by substitutions at positions in helix TH 5, 7, or 9 at residues 280, 311, and 356, respectively. Cys at these positions are readily labeled with fluorescent probes, and the labeled Cys do not prevent proper T domain membrane insertion (*28, 30*).

T domains containing the charged substitutions noted above (together with the Cys substitution at residue 356) maintained a normal ability to bind to and insert into lipid vesicles, as judged by the blue shift in T domain native Trp fluorescence upon association with lipid vesicles at low pH, and its dependence upon lipid concentration (*5*) (data not shown). We also found that the A282R/V283R mutation did not alter the pH (about 5.5) at which the toxin switches from the native neutral pH conformation to the membrane-inserting low pH form, and that, as judged by circular dichroism, T domain secondary structure was not significantly altered by the mutations (data not shown).

Effects of the Charged Mutations on the Depth of Insertion of T Domain Hydrophobic Helices as Measured by Bimane Fluorescence Wavelength. Bimane emission fluorescence is very sensitive to the polarity of its environment. A Cys deeply buried in the lipid bilayer gives more blue-shifted bimane fluorescence than one exposed to aqueous solution (*5, 30, 38*). For this reason, bimane λ_{max} has been useful to estimate changes in the membrane penetration depth of T domain helices (*5, 28, 30*). We measured bimane λ_{max} under two sets of conditions. In one (a low concentration of T domain inserted into DOPC-containing SUV) wild type T domain forms the P state, in which all T domain helices are only shallowly located on the membrane surface (*5, 28, 30*). In the other set of conditions (T domain inserted into DMoPC-containing SUV, a high concentration of T domain inserted DOPC-containing SUV, or T domain inserted into DOPC-containing SUV in the presence of molten globule state proteins, e.g., human serum albumin (HSA)), wild type T domain forms the TM conformation, in which TH 8−9 form a transmembrane hairpin and in which TH 5−7 deeply insert in the membrane, but in a non-TM conformation (*5, 28, 30, 38*).

Bimane fluorescence λ_{max} data for the T domain mutants studied under all of these conditions are listed in Table 1. In agreement with previous studies, in the absence of charged substitutions, all three Cys residues, A280C, G311C, and A356C, show long (red-shifted) bimane emission λ_{max} in the P state and shorter (blue-shifted) bimane emission λ_{max} in the TM state (*5, 30*). This pattern was altered in the presence of charged substitutions. Table 1 shows that introduction of the A282R/V283R mutations does not completely prevent

Table 1: Effects of Insertion-Inhibiting Mutations on the Membrane Penetration of Residues in T Domain Hydrophobic Helices as Measured by the Emission λ_{max} of Bimane-Labeled Cysteine Residues[a]

	$\lambda_{max,P}$	$\lambda_{max,TM}$			$\lambda_{max,TM}$		
T domain mutations	DOPC	DMoPC	HSA	HT	average	$\Delta\lambda_{max}$	% $\Delta\lambda_{max}$
A280C	470	461	458	464	461	9.0	100
A282R/V283R/A280C	472	468	464	469	467	5.0	56
L307R/A280C	464	461	457	464	460.7	3.3	[37][b]
G311C	465	462	458	458	459.3	5.7	100
A282R/V283R/G311C	464	459	457	458	458	6.0	105
L307R/G311C[c]	466	465	464.5	465	464.8	1.2	18
A356C	466	456	455	456	455.7	10.3	100
A282R/V283R/A356C	466	458.5	458.5	460	459	7.0	68
L307R/A356C[c]	468	459	461	460	460	8.0	94
I364K/A356C	470	468	468	469	468.3	1.7	17

[a] Samples contained 1 μg/mL T domain mutants and SUV composed of 200 μM 70% DOPC (or DMoPC when indicated)/30% DOPG in Tris-acetate buffer at pH 4.5. Labeling site mutation Cys280 is in TH 5, Cys311 is in TH 6/7, and Cys356 is in TH 9. In the presence of DOPC-containing SUV under these conditions, T domain ordinarily forms the P state, and bimane λ_{max} is defined as $\lambda_{max,P}$. In the conditions in which WT domain forms the TM state (DMoPC-containing vesicles or DOPC containing vesicles with either 5 μg/mL HSA or 5 μg/mL additional wild type T domain), bimane λ_{max} is defined as $\lambda_{max,TM}$. The three TM state λ_{max} values were averaged to derive $\lambda_{max,TM}$ average. $\Delta\lambda_{max} = \lambda_{max,\,P} - \lambda_{max,TM}$ average. The $\%\Delta\lambda_{max}$ is the value of $\Delta\lambda_{max}$ for a labeled protein in the presence of the charged mutation(s) normalized to that of the corresponding T domain lacking the charged substitutions. The results shown are for the average of two samples. The reproducibility of the λ_{max} values in duplicates was generally $\pm$ 1 nm. [b] This number is low because of the change in the emission of bimane in the P state. Under TM state conditions, this protein behaves in a manner similar to that of the T domain with only the A280C substitution. [c] Data from ref *39*.

the formation of a deeply inserted state by TH 5, as shown by the 5 nm blue shift in the λ_{max} of bimane-labeled residue 280 under conditions that normally allow the TM state to form relative to λ_{max} under conditions that induce formation of the P state. However, bimane λ_{max} is more red-shifted in TM state-promoting conditions than for T domain lacking these charged residues, with a 6 nm red shift of the fluorescence of bimane-labeled residue 280 relative to that in the T domain without these charged residues. This indicates that these charged residues result in shallower insertion of TH 5 under TM state-promoting conditions. In the presence of these mutations there is also somewhat shallower insertion of the TH 8−9 hairpin in the TM state, as shown by a 3 nm red shift in the fluorescence of bimane-labeled residue 356 relative to that in T domain lacking the charged mutations. In contrast, the A282R/V283R mutations do not affect the deep insertion of bimane-labeled residue 311 in the TM state. This suggests that the proper insertion of TH 5 is not absolutely required for the deep insertion of TH 6/7 (however, see below).

The behavior of T domain carrying the L307R mutation differed from that of T domain carrying the A282R/V283R mutations. Previously reported data shows that the L307R mutation causes a bimane λ_{max} red shift of bimane-labeled residue 311 under conditions that normally result in fromation of the TM state (*39*), indicating shallow TH 6/7 insertion in the presence of this charged residue. In addition, it was previously found that the L307R mutation had no effect on the fluorescence of bimane-labeled residue 356, suggesting that altered insertion of TH 6/7 has little effect upon the insertion of TH 8/9. The data in Table 1 shows that the L307R mutation also has no effect on the λ_{max} of bimane-labeled residue 280 in the TM state, consistent with blocked deep insertion of TH 6/7 not affecting insertion of TH 5. However, this mutation does induce a 6 nm blue shift in the fluorescence of bimane-labeled residue 280 under conditions in which the shallower P state forms. This suggests that there is an interaction of TH 5 and TH 6/7 in the P state.

We also examined the effect of introducing a charged residue at position 364. It was previously shown by Cabiaux et al. (*42*) that the I364K substitution strongly inhibits DT toxicity. Table 1 shows that under conditions that favor the formation of the TM state the fluorescence of bimane-labeled residue 356 is strongly red-shifted in the presence of the I364K mutation relative to that in the T domain lacking this substitution. This observation indicates that the I364K mutation strongly disrupts deep insertion of the TH 8−9 helical hairpin.

It was possible that labeling with bimane altered the behavior of the T domain such that the charged mutations only prevented deep insertion when the protein was fluorescently labeled. As a control, we studied the effect of the mutations upon the degree of helix burial within the membrane by measuring the accessibility of the protein to labeling with N-ethyl maleimide (NEM). It has been shown that NEM reactivity is greater for Cys residues exposed to solution than for Cys residues that are buried within the membrane (*43–45*). Under conditions that promote formation of the TM state, we found that the relative rate of reaction with ^{14}C-NEM for a Cys at position 280, 311, or 356 increased 1.8-fold, 2.6-fold, and-1.4 fold, respectively, in the presence of the A282R/V283R mutation, L307R mutation, or I364K mutation, respectively (data not shown). Therefore, the shallower location of these Cys residues in the presence of a nearby charged mutation is not due to the presence of a fluorescent label.

Effects of Charged Mutations on the Depth of Insertion of T Domain Helices as Measured by 10-DN/Iodide Dual Quenching. A dual quenching method (*23, 39, 46*) was used to help confirm the location of the fluorescently labeled bimane residues. In this method, 10-DN, which is a bilayer-inserted hydrophobic quencher (*41*), most efficiently quenches the fluorescence of bimane-labeled residues exposed to the hydrophobic core of the bilayer, while iodide, a hydrophilic quencher that predominantly resides in the aqueous solution, most efficiently quenches the fluorescence of bimane exposed

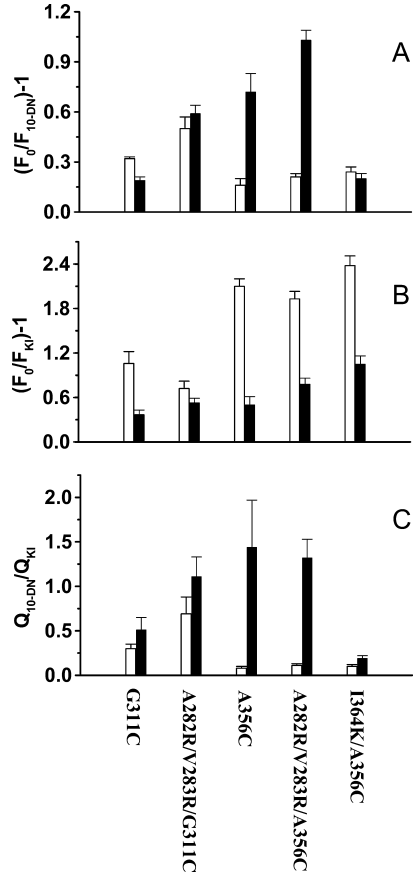

FIGURE 1: 10-DN and iodide quenching of bimane-labeled T domain. Samples contained SUV composed of 200 μM 70% PC/30% DOPG with or without 10-DN (see Experimental Procedures) and 1μg/mL bimane-labeled T domain in Tris-acetate buffer at pH 4.5. (A) Quenching by 10-DN. (B) Quenching by KI. (C) Ratio of quenching by 10-DN to that of KI. Open bars indicate quenching under conditions that promote the formation of the P state (DOPC-containing SUV); closed bars indicate conditions promoting the formation of the TM state (DMoPC-containing SUV). F_0 is the bimane fluorescence in the absence of quencher; $F_{10\text{-}DN}$ and F_{KI} are the bimane fluorescence in the presence of 10-DN or KI, respectively. Values shown are in A and B, the average of two samples and the upper limit of their range (average deviation) or in C, the ratio of the average values in A and B and the product of the quenching ratio and the sum of the relative average deviations (average deviation/quenching value).

to aqueous solution. The ratio of quenching by these two probes is a good measure of the depth of burial of a bimane-labeled residue within the lipid bilayer (*23, 39, 46*).

In agreement with our previous studies, Figure 1 shows that in the T domain lacking charged substitutions bimane-labeled G311C and A356C exhibit a lower quenching ratio in DOPC vesicles (P state) and a higher quenching ratio in DMoPC vesicles (TM state), consistent with these residues having a shallower location in the bilayer in the P state and a deeper location in the bilayer in the TM state. [Data for bimane-labeled residue 280 is not shown because we found that 10-DN can induce a conformational change in TH 5. Supporting this conclusion, under conditions in which the TM conformation usually forms, the λ_{max} of the fluorescence emission of bimane-labeled residue 280 in the presence of 10-DN red-shifted, indicating that the P conformation had formed (data not shown). In addition, instead of quenching, there was an increase in fluorescence in the presence of the quencher.]

Figure 1 shows that in the presence of the A282R/V283R mutation TH 6/7 insertion is not inhibited as judged by the depth of bimane-labeled residue 311. This agrees with bimane λ_{max} data. In fact, as judged by quenching, the labeled 311 residue appears to insert slightly more deeply in both the P and TM states in the presence of the A282R/V283R mutation than in its absence. There is a hint of this behavior in the λ_{max} of labeled 311, which is slightly more blue-shifted in the presence of the A282R/V283R mutation than in its absence (Table 1).

Quenching also shows that under conditions that normally promote the formation of the TM state there is at most only a small decrease in the depth of bimane-labeled residue 356 in the presence of the A282R/V283R mutation. In contrast, quenching indicates the I364K mutation prevents deep insertion of bimane-labeled residue 356, in excellent agreement with the large red shift in λ_{max} in the presence of this mutation relative to that in the T domain lacking this substitution under conditions that normally promote formation of the TM state.

Effects of Charged Mutations on the Depth of Insertion of T Domain Helices as Measured by Antibody-Induced Quenching of BODIPY Fluorescence. The effect of charged mutations upon the exposure of BODIPY-labeled residues to anti-BODIPY antibodies was also measured. This assay makes use of the observation that when antibodies bind to BODIPY groups they partially quench BODIPY fluorescence (*5, 28, 30*). Thus, solution-exposed residues can be distinguished from those buried in the membrane, which are not very accessible to antibody. This method does not measure exactly the same parameter as bimane fluorescence or bimane quenching because residues that are membrane-inserted in a dynamic fashion, such that they equilibrate between a predominantly deeply inserted state and less abundant shallowly inserted state, could bind antibodies during the brief periods that they become solution-exposed.

BODIPY antibody-induced quenching results are listed in Table 2. T domains carrying only a single Cys mutation, A280C, G311C, or A356C, show strong quenching in the P state and decreased quenching in the TM state, indicating that the sequences in which they are located, TH 5, TH 6/7 and TH 9, respectively, locate shallowly in the P state and deeply in the TM state, in agreement with previous studies and bimane fluorescence (*5, 28, 30*).

Table 2 shows that in the case of T domain containing a BODIPY-labeled Cys 280 and the A282R/V283R mutations in TH 5 there is no decrease in antibody-induced quenching in the TM state-promoting conditions relative to P state-promoting conditions. This is in contrast to what is observed with a wild type sequence at residues 282 and 283 and indicates that the A282R/V283R mutation destabilizes the deep insertion of TH 5, in agreement with the bimane λmax data described above.

Antibody-induced quenching also indicates that the A282R/V283R mutations also destabilized deep insertion of BODIPY-labeled residue 356, but only to a small degree. This is also in agreement with bimane λ_{max} data described above.

In addition, Table 2 shows that as judged by antibody-induced quenching the A282R/V283R mutations destabilize deep insertion of BODIPY-labeled residue 311 to a significant degree. This is surprising because the 282/283 substitutions did not result in the shallower insertion of residue 311

Table 2: Effects of the Insertion-Inhibiting Mutations on the Membrane Penetration of Residues in T Domain Hydrophobic Helices as Measured by Antibody Quenching of BODIPY Fluorescence[a]

	$\%Q_P$	$\%Q_{TM}$				
T domain mutations	DOPC	DMoPC	HSA	HT	average %ΔQ	normalized %ΔQ
A280C	47.4 ± 4.9	20.2 ± 4.2	17.4 ± 2.6	19.1 ± 1.7	60	100
A282R/V283R/A280C	31.0 ± 3.6	29.3 ± 1.3	27.6 ± 1.0	31.6 ± 1.2	5	8.0
L307R/A280C	56.6 ± 2.4	33.6 ± 1.8	18.5 ± 2.1	25.5 ± 1.9	54	90
G311C	40.5 ± 2.9	11.4 ± 1.7	9.4 ± 1.5	9.9 ± 3.5	75	100
A282R/V283R/G311C	39.4 ± 1.2	21.0 ± 1.3	17.3 ± 2.4	24.7 ± 1.3	47	62
L307R/G311C[b]	41.7 ± 4.5	19.7 ± 3.7	30.0 ± 3.8	26.0 ± 0.0	40	53
A356C	44.8 ± 1.6	8.4 ± 1.6	9.6 ± 1.4	10.5 ± 1.8	79	100
A282R/V283R/A356C	49.0 ± 2.0	15.9 ± 2.5	14.0 ± 0.9	18.8 ± 1.5	67	85
L307R/A356C[b]	35.3 ± 0.4	17.7 ± 1.0	22.7 ± 1.2	17.6 ± 1.4	45	[83][c]
I364K/356C	55.9 ± 2.0	47.9 ± 1.8	46.6 ± 0.1	49.4 ± 1.1	14	18

[a] Sample composition as in Table 1, except that protein is BODIPY-labeled. The percent quenching of BODIPY fluorescence intensity under P state-promoting conditions ($\%Q_{P,DOPC}$) and the percent quenching under TM state-promoting conditions ($\%Q_{TM,\ DMoPC}$, $\%Q_{TM,\ HSA}$, $\%Q_{TM,HT}$) were used to calculate the average %ΔQ, using the formula average $\%\Delta Q = (\%Q_{P,DOPC} - (\%Q_{TM,\ DMoPC} + \%Q_{TM,\ HSA} + \%Q_{TM,HT})/3)/\ \%Q_{P,DOPC}) \times 100\%$. Normalized $\%\Delta Q = \%\Delta Q/\%\Delta Q$ for the corresponding labeled T domain lacking charged substitution(s), unless otherwise noted. The average values from two samples and the range are shown. [b] Data from ref *39*. [c] This value of %ΔQ relative to A356C T domain values is from previously published data (*39*). The antibody preparation used in the previous study gave weaker quenching of the BODIPY-labeled A356C T domain.

in TM state-promoting conditions as judged by bimane λ_{max} or dual quenching. This suggests that in the presence of these charged substitutions either the deep insertion of BODIPY-labeled residue 311 under conditions that promote formation of the TM state is sufficiently dynamic so that labeled residue 311 can react with antibody in the aqueous solution or that the BODIPY-labeled residue 311 does not insert as deeply in the TM state as bimane-labeled residue 311.

In contrast, antibody-induced quenching indicates the L307R mutation has at most only a small effect on the stability of the deep insertion of BODIPY-labeled residue 280. This is in agreement with the highly blue-shifted fluorescence of bimane-labeled residue 280 observed in the presence of the L307R mutation under conditions promoting the formation of the TM state.

However, under conditions promoting formation of the P state there is a difference in BODIPY and bimane label behavior for labeled residue 280 in the presence of the L307R mutation. As judged by quenching, BODIPY-labeled residue 280 is more accessible to antibody in the presence of the L307R mutation than in its absence, while bimane-labeled residue 280 showed fluorescence that is more blue-shifted than in the absence of the L307R mutation. This suggests either that the unusual deep insertion observed in the P state in the presence of the L307R mutation is dynamic so that labeled residue 280 can readily react with antibody in the aqueous solution or that under conditions that normally induce formation of the P state in, the presence of the L307R mutation the BODIPY-labeled residue 280 does not insert as deeply as does as bimane-labeled residue 280.

Finally, Table 2 shows that, as judged by antibody-induced quenching, the presence of the I364K mutation strongly destabilizes deep insertion of BODIPY-labeled residue 356 under conditions that normally promote the formation of the TM state in agreement with both bimane λ_{max} and dual quenching results.

Effects of Insertion-Inhibiting Mutations on Pore Formation. The formation of pores within the lipid bilayer is an important property of the T domain and is strongly correlated with the deep insertion of T domain helices 8 and 9 (*17*). In the open channel state, in which the C-terminal hydrophilic helices have translocated across the bilayer to the trans solution, helix 8 and 9 appear to be sufficient for normal pore formation (*33*). However, the structure of the pore is not completely defined in the TM conformation, which is a pretranslocated state in which the C-terminal hydrophilic helices have not translocated and remain associated with the cis surface of the membrane (*23*).

To examine this subject, we assayed pore formation in the presence of the insertion-disrupting mutations. We used the biocytin influx method recently developed in our laboratory to detect pores formed by the T domain (*39*). In this method, BODIPY-streptavidin (SA) is trapped in the lumen of large unilamellar vesicles. T domain is added externally, and after its insertion into the lipid bilayer at low pH, biocytin (biotinyl-Lys) is added. The influx of biocytin results in its binding to BODIPY-SA, which is detected by a large increase in BODIPY fluorescence. This method has the advantage that influx can be initiated long after T domain insertion so that any transient permeability that accompanies T domain insertion does not interfere with the detection of true pore formation.

Figure 2 shows the time course of the BODIPY-SA fluorescence increase due to biocytin influx into vesicles in which the T domain is inserted. The rate of influx is greatest for the "wild-type" protein (i.e., lacking any insertion-blocking mutations) and for T domain with the L307R mutation. The lack of inhibition of pore formation by the L307R mutant is consistent with our previous studies (*31, 39*) and indicates that deep insertion of TH 6/7 is not required for pore formation. In fact, it appears that the L307R mutation enhances pore formation. In contrast, T domain carrying the A282R/V283R mutations shows a decreased ability to form pores relative to the T domain without charged substitutions. This suggests that blocking the insertion of TH 5 directly or indirectly inhibits pore formation (see Discussion). It also supports the conclusion that this mutation alters the insertion of TH 5 even when the protein is not labeled with a fluorescent probe. The greatest inhibition of pore formation is observed for the I364K mutation. This supports the conclusion that the I364K mutation blocks TH 9 insertion.

Figure 3 illustrates the concentration dependence of the average rate of biocytin influx induced by wild type and mutant T domains. The order of the differences in the influx rate for wild type protein and various mutants is not dependent upon the concentration of the T domain. In all

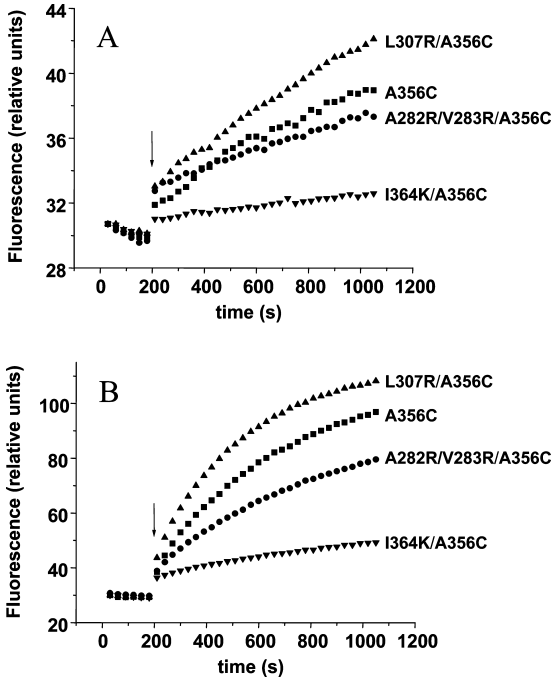

FIGURE 2: Time dependence of T domain induced pore formation at pH 4.5. Samples contained LUV composed of 100 μM 70% DOPC/30% DOPG with 90 ng/mL trapped BODIPY-streptavidin and (A) 0.22 μg/mL or (B) 0.88 μg/mL T domain preincubated in Tris-acetate buffer at pH 4.5 for 20 min. BODIPY fluorescence was recorded after the addition of 30 nM biocytin (arrow). Symbols indicate T domain containing the A356C mutation and (■) no charged substitution ("WT"); (●) A282R/V283R substitutions; (▲) L307R substitution; and (▼) I364K substitution. The presence of the A356C mutation does not greatly affect pore formation (data not shown).

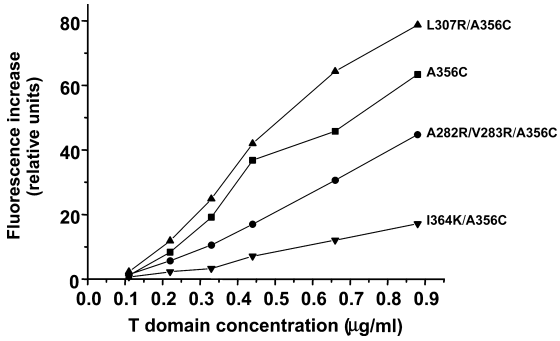

FIGURE 3: Protein concentration dependence of T domain-induced pore formation. Samples are as described in Figure 2 except that T domain concentration was varied as shown. The *y*-axis shows the fluorescence signal increase over the first 1020 s after the addition of biocytin. This average rate parameter was measured because initial rates were hard to estimate at low T domain concentrations. Symbols indicate T domain containing the A356C mutation and (■) no charged substitution ("WT"); (●) A282R/V283R substitutions; (▲) L307R substitution; and (▼) I364K substitution. The data shown is for single samples.

cases, the rate of influx increases with increasing T domain concentration. This could mean that either the number of pores is increasing or the pore size is increasing. In this regard it is noteworthy that the dependence upon T domain concentration is nonlinear such that lower T domain concentrations are unable to induce significant pore formation. This is indicative of an increase in pore size at higher T domain concentrations, presumably due to oligomerization, in agreement with our previous studies (*47*). The observation that the effects of the charged mutations are similar at low and high T domain concentration suggest that the effects of these mutations are not dependent upon T domain oligomeric state (*47*).

DISCUSSION

Using Insertion-Blocking Mutations to Characterize the Tertiary Structure of Membrane-Inserted T Domain and T Domain Pore Formation: Effect of Inhibition of TH 5 Insertion. Membrane-inserted diphtheria toxin T domain has unusual physical properties. It can exist in a number of topographies at different stages of translocation (*14, 16, 23, 30, 31*) and as a result the degree to which different helices interact with each other is not as well-defined as for normal TM proteins. As noted in the Introduction, insertion-blocking mutations have been useful to map out T domain helix insertion, helix−helix interaction, and pore formation. Prior studies showed that blocking the proper insertion of TH 8−9 prevents deep insertion of TH 5 and TH 6/7, while blocking deep insertion of TH 6/7 has no effect on the insertion of TH 8−9 (*39*).

The behavior of T domain carrying the A282R/V283R mutations within TH 5 provides new insights into the interaction of TH 5 with other T domain hydrophobic helices. These mutations block the deep insertion of TH 5 to a substantial degree. They have a much smaller effect upon the deep insertion of TH 6/7. Since there is also little effect of blocking TH 6/7 deep insertion on the deep insertion of TH 5, it appears that TH 5 and TH 6/7 do not interact strongly with each other when the T domain is in the deeply inserted TM state, although they may in the P state (see below). Blocking TH 5 deep insertion with these mutations also decreased the deep insertion of TH 8−9 to a significant degree.

It was also found that blocking the insertion of TH 5 inhibited the extent of T domain-induced pore formation to a significant degree. This might mean that TH 5 directly participates in the formation of the pore in the pretranslocation TM state. Alternately, preventing the deep insertion of TH 5 may indirectly affect pore formation by affecting the conformation of TH 8−9. Combining these results with the previous observation that blocking the insertion of TH 8−9 also blocks the deep insertion of TH 5 (*39*) indicates that TH 5 and TH 8−9 form a cluster of interacting helices in the TM state (see below).

Effect of Inhibition of TH 6/7 Insertion. The interaction of TH 6/7 with TH 8−9 was studied with the L307R mutation. As noted above, it was shown previously that the L307R mutation blocked the deep insertion of TH 6/7 but not the deep insertion of TH 8−9 (*39*). We now find that the L307R mutation also fails to block the deep insertion of TH 5.

However, there may be a more intimate interaction between TH 5 and TH 6/7 in the shallowly inserted P state because blocking the deep insertion of TH 6/7 resulted in the deeper insertion of TH 5 in the P state, at least as judged by the fluorescence emission of bimane-labeled residue 280.

The effect of the L307R mutation on pore formation is interesting. Blocking the deep insertion of TH 6/7 appeared to enhance the extent of pore formation. This is consistent with a model in which deeply inserted TH 6/7 may partly

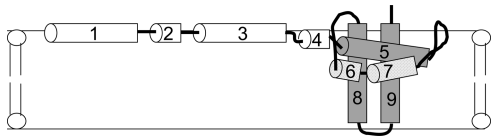

FIGURE 4: Schematic figure illustrating the hierarchy of interactions between T domain helices. Deep insertion of darkly shaded helices is mutually interdependent. Deep insertion of lightly shaded helices is dependent on the deep insertion of darkly shaded helices. Insertion of unshaded helices is not strongly affected by the deep insertion of shaded helices.

block pore formation by forming a "plug" or "cork". Combined with the effects of blocking the deep insertion of TH 5 upon pore properties, this suggests that there are significant differences between the pore properties of the membrane-inserted pretranslocation state and the membrane-inserted post-translocation state. Perhaps this should not be surprising given the difference in topography of these two states (*16, 23, 30, 31*).

Effect of Inhibition of TH 8−9 Insertion. The behavior of the I364K mutation is particularly interesting because it has been shown by Cabiaux et al. that this mutation strongly inhibits toxicity and pore formation when introduced into *whole* DT (*42*). It was hypothesized that blocked insertion of TH 9 might be responsible for the effects of this mutation. Our studies show that this mutation does indeed block the deep insertion of TH 9 as well as pore formation by *isolated*T domain and thus supports the hypothesis of Cabiaux et al.

Model of T Domain Topography, Helix−Helix Interactions and Pore Formation in the Deeply Inserted Pre-Translocation TM State. Combining the results above and the previous results allows us to formulate a model for the interactions between T domain hydrophobic helices in the TM state (Figure 4). There appears to be a hierarchy in which TH 5, 8, and 9 interact strongly such that their deep insertion is mutually interdependent. In contrast, although the deep insertion of TH 6/7 is dependent on that of TH 8−9 and perhaps that of THS the deep insertion of TH 5, 8, and 9 are not dependent on the deep insertion of TH 6/7. In other words, deeply inserted TH 5, 8, and 9 form some sort of scaffold, with which TH 6/7 interacts more loosely (Figure 4).

It also appears that TH 5, 8, and 9 cooperate to form the T domain pore, although it is not certain whether TH 5 directly participates in forming the walls of the pore. As noted above, the observation that TH 6/7 limits the extent of pore formation suggests that it may partly plug the pore. Because TH 6/7 is a moderately hydrophobic sequence, this would be consistent with our previous hypothesis that the pore formed by the T domain recognizes somewhat hydrophobic sequences and proteins, including the partly unfolded A chain, as part of a chaperone-like function during translocation (*37, 38, 48*). TH 6/7 interactions with the pore could be analogous to pseudosubstrate type of behavior. If this is true, significant conformational changes in the pretranslocation state of the T domain may be necessary to form the final pore/pathway through which the A chain translocates. Further dissecting the complex conformational changes that accompany DT-induced translocation should provide crucial insights into the mechanism of protein translocation, for both DT and other protein toxins.

REFERENCES

1. Choe, S., Bennett, M. J., Fujii, G., Curmi, P. M., Kantardjieff, K. A., Collier, R. J., and Eisenberg, D. (1992) The crystal structure of diphtheria toxin. *Nature 357*, 216–222.
2. Bennett, M. J., and Eisenberg, D. (1994) Refined structure of monomeric diphtheria toxin at 2.3 Å resolution. *Protein Sci. 3*, 1464–1475.
3. Bennett, M. J., Choe, S., and Eisenberg, D. (1994) Refined structure of dimeric diphtheria toxin at 2.0 Å resolution. *Protein Sci. 3*, 1444–1463.
4. Zhan, H., Oh, K. J., Shin, Y. K., Hubbell, W. L., and Collier, R. J. (1995) Interaction of the isolated transmembrane domain of diphtheria toxin with membranes. *Biochemistry 34*, 4856–4863.
5. Wang, Y., Malenbaum, S. E., Kachel, K., Zhan, H., Collier, R. J., and London, E. (1997) Identification of shallow and deep membrane-penetrating forms of diphtheria toxin T domain that are regulated by protein concentration and bilayer width. *J. Biol. Chem. 272*, 25091–25098.
6. Wang, Y., Kachel, K., Pablo, L., and London, E. (1997) Use of Trp mutations to evaluate the conformational behavior and membrane insertion of A and B chains in whole diphtheria toxin. *Biochemistry 36*, 16300–16308.
7. Moskaug, J. O., Stenmark, H., and Olsnes, S. (1991) Insertion of diphtheria toxin B-fragment into the plasma membrane at low pH. Characterization and topology of inserted regions. *J. Biol. Chem. 266*, 2652–2659.
8. Hu, V. W., and Holmes, R. K. (1984) Evidence for direct insertion of fragments A and B of diphtheria toxin into model membranes. *J. Biol. Chem. 259*, 12226–12233.
9. Falnes, P. O., and Sandvig, K. (2000) Penetration of protein toxins into cells. *Curr. Opin. Cell Biol. 12*, 407–413.
10. London, E. (1992) Diphtheria toxin: membrane interaction and membrane translocation. *Biochim. Biophys. Acta 1113*, 25–51.
11. Ratts, R., Trujillo, C., Bharti, A., vanderSpek, J., Harrison, R., and Murphy, J. R. (2005) A conserved motif in transmembrane helix 1 of diphtheria toxin mediates catalytic domain delivery to the cytosol. *Proc. Natl. Acad. Sci. U.S.A. 102*, 15635–15640.
12. Pappenheimer, A. M., Jr. (1977) Diphtheria toxin. *Annu. Rev. Biochem. 46*, 69–94.
13. Finkelstein, A., Oh, K. J., Senzel, L., Gordon, M., Blaustein, R. O., and Collier, R. J. (2000) The diphtheria toxin channel-forming T-domain translocates its own NH2-terminal region and the catalytic domain across planar phospholipid bilayers. *Int. J. Med. Microbiol. 290*, 435–440.
14. Montagner, C., Perier, A., Pichard, S., Vernier, G., Menez, A., Gillet, D., Forge, V., and Chenal, A. (2007) Behavior of the N-terminal helices of the diphtheria toxin T domain during the successive steps of membrane interaction. *Biochemistry 46*, 1878–1887.
15. Oh, K. J., Senzel, L., Collier, R. J., and Finkelstein, A. (1999) Translocation of the catalytic domain of diphtheria toxin across planar phospholipid bilayers by its own T domain. *Proc. Natl. Acad. Sci. U.S.A. 96*, 8467–8470.
16. Senzel, L., Huynh, P. D., Jakes, K. S., Collier, R. J., and Finkelstein, A. (1998) The diphtheria toxin channel-forming T domain translocates its own NH2-terminal region across planar bilayers. *J. Gen. Physiol. 112*, 317–324.
17. Zhan, H., Elliott, J. L., Shen, W. H., Huynh, P. D., Finkelstein, A., and Collier, R. J. (1999) Effects of mutations in proline 345 on insertion of diphtheria toxin into model membranes. *J. Membr. Biol. 167*, 173–181.
18. Ladokhin, A. S., Legmann, R., Collier, R. J., and White, S. H. (2004) Reversible refolding of the diphtheria toxin T-domain on lipid membranes. *Biochemistry 43*, 7451–7458.
19. Palchevskyy, S. S., Posokhov, Y. O., Olivier, B., Popot, J. L., Pucci, B., and Ladokhin, A. S. (2006) Chaperoning of insertion of membrane proteins into lipid bilayers by hemifluorinated surfactants: application to diphtheria toxin. *Biochemistry 45*, 2629–2635.
20. Perier, A., Chassaing, A., Raffestin, S., Pichard, S., Masella, M., Menez, A., Forge, V., Chenal, A., and Gillet, D. (2007) Concerted protonation of key histidines triggers membrane interaction of the diphtheria toxin T domain. *J. Biol. Chem. 282*, 24239–24245.
21. Chenal, A., Savarin, P., Nizard, P., Guillain, F., Gillet, D., and Forge, V. (2002) Membrane protein insertion regulated by bringing electrostatic and hydrophobic interactions into play. A case study with the translocation domain of diphtheria toxin. *J. Biol. Chem. 277*, 43425–43432.

22. D'Silva, P. R., and Lala, A. K. (2000) Organization of diphtheria toxin in membranes. A hydrophobic photolabeling study. *J. Biol. Chem. 275*, 11771–11777.
23. Wang, J., Rosconi, M. P., and London, E. (2006) Topography of the hydrophilic helices of membrane-inserted diphtheria toxin T domain: TH1-TH3 as a hydrophilic tether. *Biochemistry 45*, 8124–8134.
24. Oh, K. J., Zhan, H., Cui, C., Hideg, K., Collier, R. J., and Hubbell, W. L. (1996) Organization of diphtheria toxin T domain in bilayers: a site-directed spin labeling study. *Science 273*, 810–812.
25. Malenbaum, S. E., Collier, R. J., and London, E. (1998) Membrane topography of the T domain of diphtheria toxin probed with single tryptophan mutants. *Biochemistry 37*, 17915–17922.
26. Kaul, P., Silverman, J., Shen, W. H., Blanke, S. R., Huynh, P. D., Finkelstein, A., and Collier, R. J. (1996) Roles of Glu 349 and Asp 352 in membrane insertion and translocation by diphtheria toxin. *Protein Sci. 5*, 687–692.
27. Huynh, P. D., Cui, C., Zhan, H., Oh, K. J., Collier, R. J., and Finkelstein, A. (1997) Probing the structure of the diphtheria toxin channel. Reactivity in planar lipid bilayer membranes of cysteine-substituted mutant channels with methanethiosulfonate derivatives. *J. Gen. Physiol. 110*, 229–242.
28. Kachel, K., Ren, J., Collier, R. J., and London, E. (1998) Identifying transmembrane states and defining the membrane insertion boundaries of hydrophobic helices in membrane-inserted diphtheria toxin T domain. *J. Biol. Chem. 273*, 22950–22956.
29. Oh, K. J., Zhan, H., Cui, C., Altenbach, C., Hubbell, W. L., and Collier, R. J. (1999) Conformation of the diphtheria toxin T domain in membranes: a site-directed spin-labeling study of the TH8 helix and TL5 loop. *Biochemistry 38*, 10336–10343.
30. Rosconi, M. P., and London, E. (2002) Topography of helices 5–7 in membrane-inserted diphtheria toxin T domain: identification and insertion boundaries of two hydrophobic sequences that do not form a stable transmembrane hairpin. *J. Biol. Chem. 277*, 16517–16527.
31. Rosconi, M. P., Zhao, G., and London, E. (2004) Analyzing topography of membrane-inserted diphtheria toxin T domain using BODIPY-streptavidin: at low pH, helices 8 and 9 form a transmembrane hairpin but helices 5–7 form stable nonclassical inserted segments on the cis side of the bilayer. *Biochemistry 43*, 9127–9139.
32. Madshus, I. H., Wiedlocha, A., and Sandvig, K. (1994) Intermediates in translocation of diphtheria toxin across the plasma membrane. *J. Biol. Chem. 269*, 4648–4652.
33. Silverman, J. A., Mindell, J. A., Zhan, H., Finkelstein, A., and Collier, R. J. (1994) Structure-function relationships in diphtheria toxin channels: I. Determining a minimal channel-forming domain. *J. Membr. Biol. 137*, 17–28.
34. Falnes, P. O., Madshus, I. H., Sandvig, K., and Olsnes, S. (1992) Replacement of negative by positive charges in the presumed membrane-inserted part of diphtheria toxin B fragment. Effect on membrane translocation and on formation of cation channels. *J. Biol. Chem. 267*, 12284–12290.
35. Mindell, J. A., Silverman, J. A., Collier, R. J., and Finkelstein, A. (1994) Structure function relationships in diphtheria toxin channels: II. A residue responsible for the channel's dependence on trans pH. *J. Membr. Biol. 137*, 29–44.
36. Mindell, J. A., Silverman, J. A., Collier, R. J., and Finkelstein, A. (1994) Structure-function relationships in diphtheria toxin channels: III. Residues which affect the cis pH dependence of channel conductance. *J. Membr. Biol. 137*, 45–57.
37. Hammond, K., Caputo, G. A., and London, E. (2002) Interaction of the membrane-inserted diphtheria toxin T domain with peptides and its possible implications for chaperone-like T domain behavior. *Biochemistry 41*, 3243–3253.
38. Ren, J., Kachel, K., Kim, H., Malenbaum, S. E., Collier, R. J., and London, E. (1999) Interaction of diphtheria toxin T domain with molten globule-like proteins and its implications for translocation. *Science 284*, 955–957.
39. Zhao, G., and London, E. (2005) Behavior of diphtheria toxin T domain containing substitutions that block normal membrane insertion at Pro345 and Leu307: control of deep membrane insertion and coupling between deep insertion of hydrophobic subdomains. *Biochemistry 44*, 4488–4498.
40. Zhan, H., Choe, S., Huynh, P. D., Finkelstein, A., Eisenberg, D., and Collier, R. J. (1994) Dynamic transitions of the transmembrane domain of diphtheria toxin: disulfide trapping and fluorescence proximity studies. *Biochemistry 33*, 11254–11263.
41. Caputo, G. A., and London, E. (2003) Using a novel dual fluorescence quenching assay for measurement of tryptophan depth within lipid bilayers to determine hydrophobic α helix locations within membranes. *Biochemistry 42*, 3265–3274.
42. Cabiaux, V., Mindell, J., and Collier, R. J. (1993) Membrane translocation and channel-forming activities of diphtheria toxin are blocked by replacing isoleucine 364 with lysine. *Infect. Immun. 61*, 2200–2202.
43. Kuwabara, N., Inoue, H., Tsuboi, Y., Mitsui, K., Matsushita, M., and Kanazawa, H. (2006) Structure-function relationship of the fifth transmembrane domain in the Na+/H+ antiporter of Helicobacter pylori: Topology and function of the residues, including two consecutive essential aspartate residues. *Biochemistry 45*, 14834–14842.
44. Venkatesan, P., Kwaw, I., Hu, Y., and Kaback, H. R. (2000) Site-directed sulfhydryl labeling of the lactose permease of Escherichia coli: helix VII. *Biochemistry 39*, 10641–10648.
45. Frillingos, S., and Kaback, H. R. (1996) Probing the conformation of the lactose permease of Escherichia coli by in situ site-directed sulfhydryl modification. *Biochemistry 35*, 3950–3956.
46. Hayashibara, M., and London, E. (2005) Topography of diphtheria toxin A chain inserted into lipid vesicles. *Biochemistry 44*, 2183–2196.
47. Sharpe, J. C., and London, E. (1999) Diphtheria toxin forms pores of different sizes depending on its concentration in membranes: probable relationship to oligomerization. *J. Membr. Biol. 171*, 209–221.
48. Zhao, J. M., and London, E. (1988) Conformation and model membrane interactions of diphtheria toxin fragment A. *J. Biol. Chem. 263*, 15369–15377.

BI7025134